The New Hybrid Product Approach: Aligning Project Specifications with UAS Photogrammetry and Lidar

Prepared by: Qassim Abdullah, Ph.D., PLS, CP, VP and Chief Scientist; and Tom Ruschkewicz, Practice Leader, Transportation

August 2021

Abstract

This paper discusses research on a new and creative method of merging geospatial data from differing backgrounds and with varied accuracy specifications. This paper discusses the following topics:

- Definition of project zones and identification of the data requirements for each zone
- Zone-specific data acquisition technology selection
- Steps for producing a hybrid product such as accuracy verification, data preparation and product development
- Case studies and project examples

This paper concludes that demand for geospatial data is increasing, and hybrid data fusion is among the best methods for producing accurate models of such information. This requires a great amount of analysis, especially in considering data accuracy, to ensure the correct approach is taken. Aside from providing evidence for the usefulness of emerging geospatial technologies in transportation projects, the benefits derived from the new hybrid product approach include cost and time savings, critical for clients with constrained budgets.

Background

Continuously declining construction project funding poses a great challenge for agencies attempting to finance new projects and/or maintain existing ones. With constrained budgets, many agencies struggle to meet their development objectives and are searching for creative ways to advance their projects. Recognizing clients' need for survivability and resilience, Woolpert researched creative methods for enabling goal achievement under strict budgets.

As the capabilities of geospatial data acquisition technologies are refined over time, more products from different sensors are able to relate to each other in terms of data quality and accuracy—making it easier for project managers and engineers to seamlessly integrate different data sources into their projects.

The term data fusion, in a general sense, is used to describe the combination of available geospatial data and is practiced only as a reaction to an immediate need or incidental data finding. The data fusion discussed in this paper is different—it focuses on the early stages during project planning and design. It describes the proactive adaptation of a data evaluation strategy to stand on the synergy between disparate data sources, making these findings the pillars for project design and cost estimation.

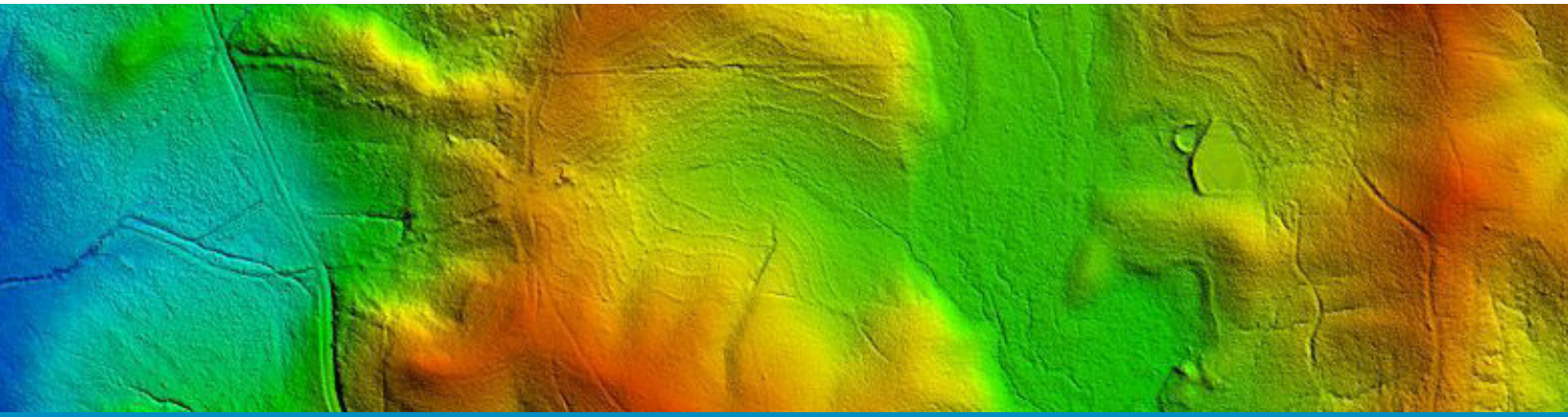

Data Specifications and Project Zoning

Today's engineers and planners can use the concept of data fusion to design their projects, saving valuable resources while assuring the promised outcome. Woolpert successfully executed projects containing varied geospatial data sources with multiple specifications acquired by different technologies, all merged to produce a seamless product that serves the planning and design phases.

Considering the requirements for planning, designing and engineering a transportation corridor (e.g., roadway construction or improvement), three types of data are needed for the project zones identified below:

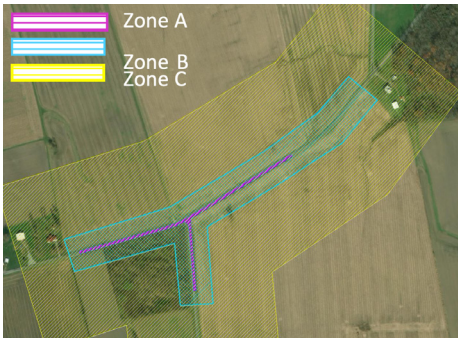

Figure 1: Zones A, B and C

Zone A: Central Region of the Right-of-Way (ROW)

Represented by zone A (Figure 1), this part of the ROW is dedicated to construction and maintenance of the main roadway and necessary outer roadways, entrances and crossroads. This region requires the most accurate geospatial data as it will be used for designing the road profile or improving the existing road. Traditionally, this area is surveyed using traditional field surveying techniques, newly contracted aerial surveys with high-resolution imagery or helicopter-based dense lidar data, as well as through lidar-based mobile mapping systems (MMS) for road improvement.

Zone B: Edges of the ROW

Represented by zone B (Figure 1), the outer limits of the ROW are reserved for utility adjustments and maintenance activities. This area's survey needs require less accuracy than that of zone A, but more than that of zone C. Traditionally, this area is surveyed using standard field surveying techniques as it is not suitable for vehicular survey equipment like MMS.

Zone C: Extended Project Basin

Represented by zone C (Figure 1) is the area surrounding the corridor path where the drainage pattern is evaluated and a hydrological model is analyzed to determine the impact of the watershed hydrography on the corridor. Depending on the roughness of the terrain, less accurate data may be suitable. Traditionally, this area is surveyed using newly contracted aerial imagery or lidar.

Technological Components

Below are the three technologies used for gathering data about the above-mentioned project zones, listed with their strengths and weaknesses.

MMS

MMS is a mapping system with a lidar sensor and multiple cameras positioned on top of a truck or van to provide 360-degree coverage of lidar data and imagery.

Strengths

MMS is the most efficient system for design-grade accuracy. It provides a detailed 3D surface (point cloud) with a density of up to 6,000 points per square meter (PPSM) and a vertical accuracy that exceeds 1 centimeter as root mean square error (RMSE).

Weaknesses

The weaknesses of MMS are its limited range (usually around 200 meters), high cost and restriction to established roadways.

Unmanned Aircraft System (UAS)

Although new, UAS is becoming an extremely versatile option for geospatial data acquisition.

Strengths

With the ability to carry lidar sensors and cameras on board, small UAS can provide high-resolution imagery ranging from 0.5- to 5-centimeter ground sampling distance (GSD) and lidar data with point density ranging from 200 to 700 PPSM. UAS is a great platform for data acquisition in zones A and B as it is a more affordable method than field surveying, MMS or even manned aircraft.

Figure 2: Imagery-derived, colorized 3D models

Weaknesses

UAS are only useful for small projects and flying over non-participants is strongly restricted by the Federal Aviation Administration (FAA). Additionally, due to its miniaturized sensors, the accuracy of the acquired data is compromised and may not be suitable for design-grade activities. This is represented in colorized 3D point clouds derived from a consumer-grade aerial camera like the one used by UAS.

Manned Aircraft

Strengths

Manned aircraft survey (lidar and imagery) is the industry workhorse for wide-area data collection. Lidar data and imagery acquired from manned aircraft sensors are available across the United States and, in most cases, are available free of charge and can be downloaded from county GIS offices.

Weaknesses

It can be costly to hire personnel for small roadway improvement projects, and limited accuracy may not support design-grade activities.

Case Study I: Petersburg/Overman Road Intersection Improvement

With the goal of improving the intersection at Petersburg and Overman roads in Highland County, OH, the data fusion approach was used to proof the project's concept (Figure 3). Woolpert used the following datasets:

- Point clouds from MMS for the road pavement (zone A)
- Point clouds and imagery from UAS for the outer limit of the ROW (zone B)
- Existing lidar data from Ohio Statewide Imagery Program (OSIP) for the area surrounding the corridor path (zone C)

Point Clouds from MMS (Zone A)

Woolpert previously conducted an MMS survey for the local transportation agency. Figures 4 and 5 illustrate the MMS point clouds for a portion of that intersection.

Figure 3: Petersburg/Overman Road intersection improvement

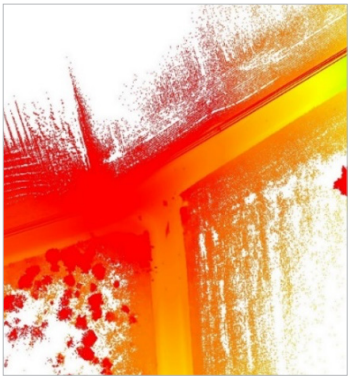

Figure 4: Point clouds from MMS (zone A)

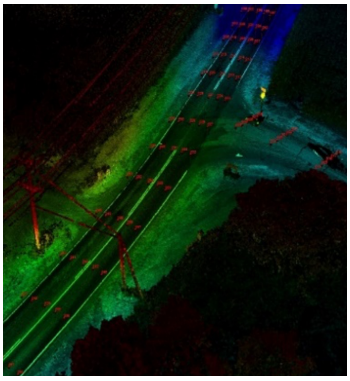

Figure 5: Point clouds from MMS (zone A) and the derived second-generation checkpoints

Point Clouds from UAS (Zone B)

The project team flew the UAS at 100 feet above ground level (AGL). Figure 6 illustrates the executed UAS flight and the ground control points used to process the data. Imagery from the UAS flight was processed using Pix4D Mapper. Figure 7 illustrates the point clouds generated from this imagery.

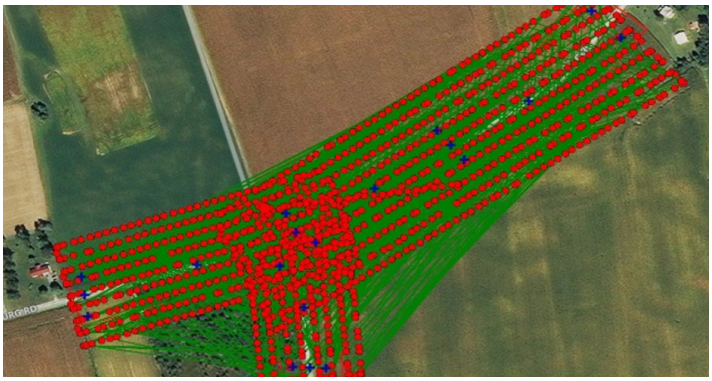

Figure 6: UAS image centers (red circles) and ground control points (blue crosses)

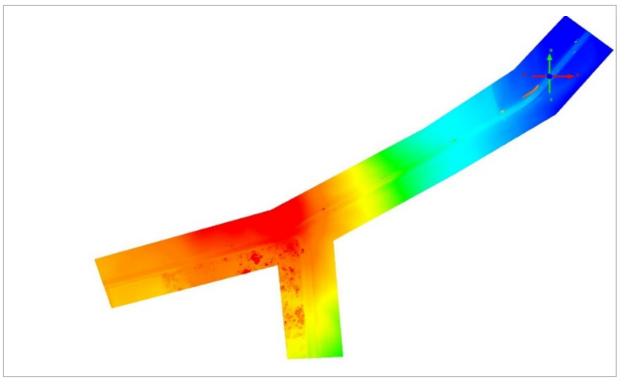

Figure 7: Point clouds generated from UAS imagery (zone B)

Lidar Point Clouds from Statewide Mapping Program (Zone C)

Lidar data for zone C was derived from OSIP and downloaded from the Ohio Geographically Referenced Information Program (OGRIP) website. Figure 8 illustrates the point clouds for this project area.

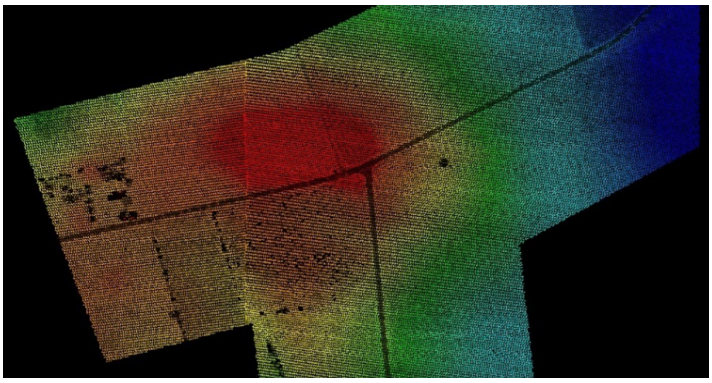

Figure 8: Lidar point clouds derived from OSIP (zone C)

Table 1: Accuracy verification results for MMS data (zone A)

Number of Check Points	79	
Mean Error	0.023 ft.	0.007 m
Standard Deviation (StDEV)	**0.037 ft.**	**0.011 m**
Root Mean Squares Error	0.043 ft.	0.013 m
NSSDA Vert Accuracy at 95%	**0.085 ft.**	**0.026 m**

Table 2: Accuracy verification results for the imagery-based DSM data, using surveyed checkpoints

Number of Check Points	73	
Mean Error	0.085 ft.	0.026 m
Standard Deviation (StDEV)	**0.130 ft.**	**0.040 m**
Root Mean Squares Error	0.154 ft.	0.047 m
NSSDA Vert Accuracy at 95%	**0.302 ft.**	**0.092 m**

Processing Steps for the Hybrid Digital Surface Model (DSM) Product

Stringent workflows should be followed when merging data to produce the hybrid DSM product. Below are the main steps for data processing:

- Accuracy verification
- Data preparation
- Product development

Accuracy Verification

One of the most important activities is verifying the positional accuracy for each product used in the generation of the hybrid product. Different products used for the hybrid DSM may have different accuracies; however, such accuracies must be independently verified and documented in the metadata of the new hybrid product.

Accuracy Verification for MMS Data

Positional vertical accuracy for the MMS data was verified using 79 checkpoints surveyed with traditional differential leveling techniques. Table 1 lists these results, reporting the MMS data was accurate to 0.043 feet (0.013 meters).

Accuracy Verification for UAS Data

Positional vertical accuracy for the UAS-derived DSM data was verified via two methods. Initially, 73 checkpoints were surveyed with traditional differential leveling techniques. Table 2 lists these results, reporting the imagery-derived DSM was accurate to 0.154 feet (0.047 meters). to the MMS data from Table 1, which the team proved accurate to 0.043 feet.

Unlike using a limited number of surveyed checkpoints, the MMS data for this type of accuracy verification provided an extensive and well-distributed network of checkpoints. In the industry, this approach is usually referred to as the second-generation checkpoint approach. Elevations of 509 locations along the road, grouped in sets of five points per cross section, were derived from the MMS DSM (Figure 5). Those 509 points were used as checkpoints to verify the accuracy of the imagery-based DSM. Table 3 lists these results, indicating the imagery-based DSM was within 0.147 feet (0.045 meters) from the MMS data.

Table 3: MMS data-derived accuracy verification results for imagery-based DSM data

Number of Check Points	509	
Mean Error	0.080 ft.	0.024 m
Standard Deviation (StDEV)	**0.124 ft.**	**0.038 m**
Root Mean Squares Error	0.147 ft.	0.045 m
NSSDA Vert Accuracy at 95% Confidence Level	**0.289 ft.**	**0.088 m**

Table 4: Accuracy verification results for OSIP lidar data

Number of Check Points	197	
Mean Error	0.474 ft.	0.144 m
Standard Deviation (StDEV)	**0.161 ft.**	**0.049 m**
Root Mean Squares Error	0.500 ft.	0.152 m
NSSDA Vert Accuracy at 95%	**0.981 ft.**	**0.299 m**

After necessary reprojection and reformatting were completed, the data went through the following steps:

Step 1
Clip MMS data to represent only roads and pavements for zone A (Figure 9).

Step 2
Clip UAS-based data to represent zone B only (Figure 10).

Step 3
Clip OSIP lidar data to represent zone C only (Figure 11).

Step 4
Merge OSIP lidar and UAS-based DSM (Figure 12).

Step 5
Merge MMS lidar, OSIP lidar and UAS-based DSM to form a seamless dataset and hybrid DSM (Figure 13).

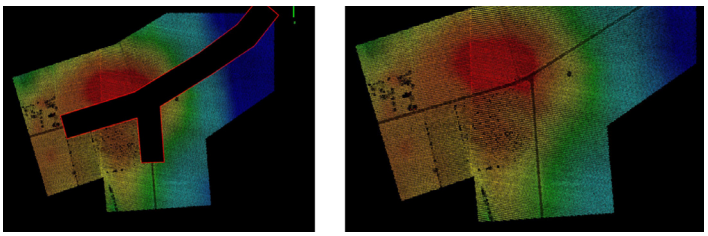

Figure 11: Zone C before and after clipping

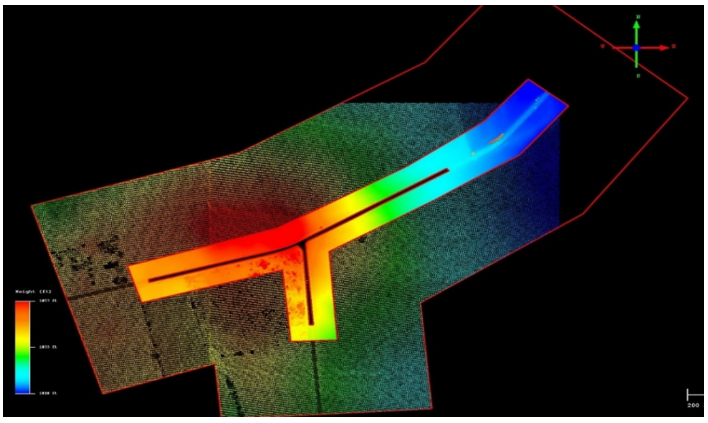

Figure 12: Merged OSIP lidar and UAS-based DSM

Accuracy Verification for OSIP Lidar Data

A total of 197 surveyed checkpoints located within zone C were used to verify the vertical accuracy of lidar data from OSIP. The metadata for the downloaded lidar data states the vertical accuracy to be 0.5 feet (15 centimeters), verified using the 197 checkpoints in Table 4.

Data Preparation

Once the project team verified the vertical accuracy of the various datasets, data processing preparations began. Data may need some, or all, of the following processing before it is merged:

- Reformatting
- Reprojecting
- Clipping and cropping

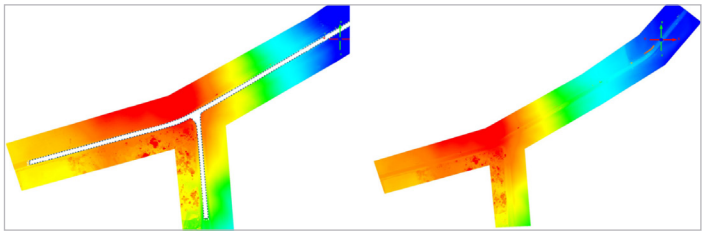

Figure 9: Zone A before and after clipping

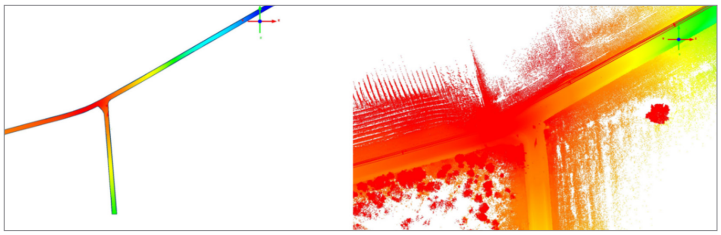

Figure 10: Zone B before and after clipping

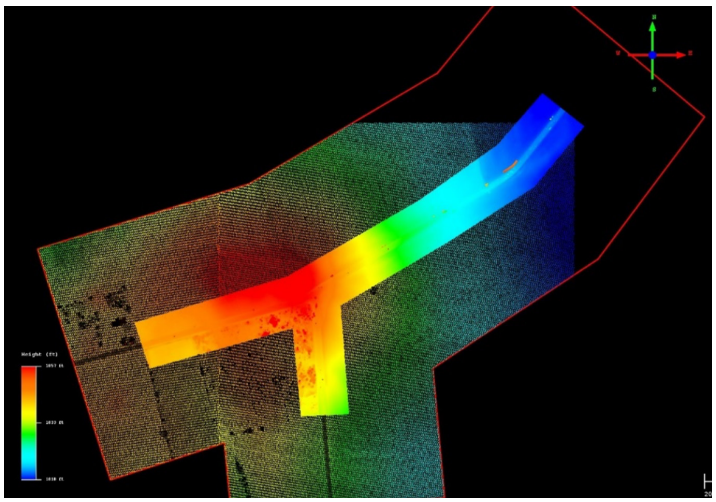

Figure 13: Hybrid DSM of three merged datasets

Product Development and Final Deliverables

After the different datasets were merged, various products could be derived for planning and design activities. Figure 14 represents one-foot contours generated from the new hybrid DSM. It is worth mentioning that although the merged datasets appear as if they are one dataset, the data within each of three zones (A, B and C) have different accuracies and should be labeled as such in the metadata (Figure 15).

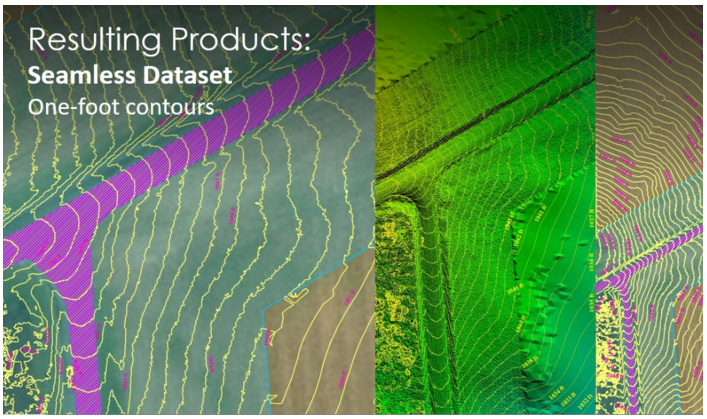

Figure 14: Seamless one-foot contours created from the hybrid DSM

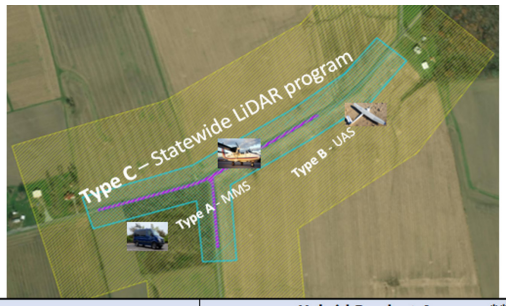

Product Specification	Hybrid Product Accuracy**		
	Type A	Type B	Type C
Terrain surface accuracy as verified using independent check points	$RMSE_v \leq 0.06$ ft.	$RMSE_v \leq 0.10$ ft.	$RMSE_v \leq 0.50$ ft.

** Type A = MMS lidar , Type B = UAS imagery-based points cloud, Type C = State wide lidar program

Figure 15: Labeled metadata associated with the hybrid DSM

Figure 16: eBee X RTK UAS flight plan and ground control points

Case Study II: UAS Proof of Concept for PennDOT

Woolpert acquired data using an eBee X RTK UAS to investigate its usefulness in supporting road design activities (Figure 16). The project team previously acquired MMS data and 7.5-centimeter imagery using a manned aircraft for section 35 of SR80 to fulfill a contract requirement with PennDOT. Imagery collected using the eBee X was used to generate the following products (Figure 17):

- Orthorectified mosaic with 2.5-centimeter GSD
- Imagery-based point clouds
- Digital terrain model (DTM)

The DTM was created with the stereophotogrammetric method, in which the stereo pairs from UAS-based imagery were used to collect the DTM for the two bounds of the freeway. The stereo pairs met the high quality expected for stereophotogrammetric mapping with no reported parallax.

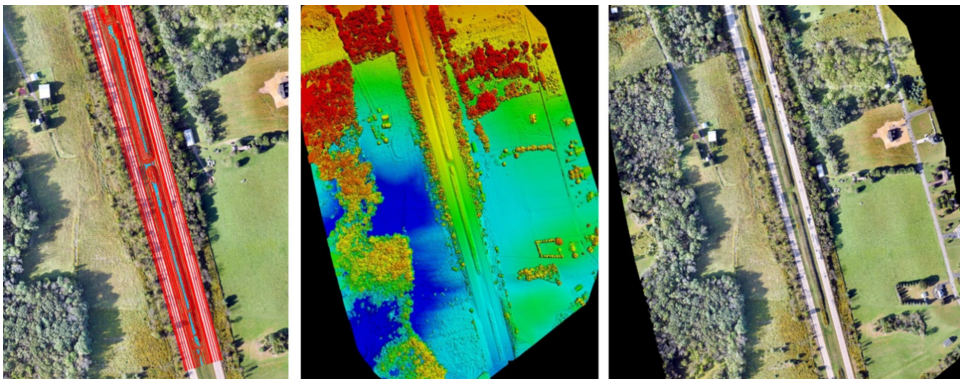

Figure 17: Products generated from UAS imagery (left: DTM; middle: point cloud; right: orthorectified mosaic)

Accuracy Verification

The vertical accuracy of the stereophotogrammetrical derived DTM was verified using the following datasets:

MMS Data

Although it has limited vertical accuracy, lidar point clouds from an accurate MMS survey can be used to verify products derived from photogrammetric techniques. Using the accuracy verification concept introduced in the first case study, the MMS data accuracy should be verified before it is used to verify the accuracy of any other dataset.

For this purpose, 28 highly accurate surveyed checkpoints provided by PennDOT were used to verify the accuracy of the MMS data. Table 5 lists the results of this accuracy verification, showing the vertical accuracy of the MMS data to be around 0.044 feet (0.013 meters).

To compare the accuracy of the compiled DTM against the MMS data, elevations for 28 checkpoints were derived along the two bounds of SR80 from the MMS data (Figure 19). Table 6 lists the results of these evaluations. From Table 6, it is evident that the UAS-based DTM had a vertical bias of around 0.224 feet. Once the bias is removed, the vertical accuracy of the UAS-based DTM was around 0.08 feet (0.025 meters). Such vertical bias is clearly seen in the profiles taken along the road (Figure 18).

Table 5: Accuracy of MMS DTM as verified using surveyed checkpoints

PennDOT UAS Proof of Concept - Accuracy Analysis (Comparing MMS DTM to PennDOT new check points)						
Note: Elevation of check points were re-projected to Geoid 12B to match the vertical datum of the data						
Point ID	Surveyed Elevation			MMS Elevation	Residual Values (ft.)	Delta Z after Z-bias Removed (ft.)
	Easting (ft.)	Northing (ft.)	Elevation (ft.)	Elevation (ft.)	Error in Elevation (ft.)	
CP_1	2447833.0894	321000.2444	1090.7890	1090.7900	-0.0010	-0.0014
CP_2	2447802.1717	321113.8212	1094.5240	1094.5600	-0.0360	-0.0364
CP_3	2447772.2693	321223.4371	1098.1050	1098.1300	-0.0250	-0.0254
CP_4	2447748.5271	321310.1031	1100.9470	1100.9800	-0.0330	-0.0334
CP_5	2447717.8919	321422.8742	1104.6990	1104.6900	0.0090	0.0086
CP_6	2447692.8522	321515.1178	1107.7650	1107.7600	0.0050	0.0046
CP_7	2447667.4935	321607.4306	1110.8140	1110.8400	-0.0260	-0.0264
CP_8	2447639.9596	321708.4858	1114.1970	1114.2000	-0.0030	-0.0034
CP_9	2447616.1907	321796.2994	1117.1080	1117.1100	-0.0020	-0.0024
CP_10	2447589.1547	321894.9876	1120.3930	1120.4200	-0.0270	-0.0274
CP_11	2447560.6492	321999.9689	1123.9770	1123.9900	-0.0130	-0.0134
CP_12	2447536.9992	322086.5782	1126.8480	1126.8800	-0.0320	-0.0324
CP_13	2447513.7209	322171.3742	1129.7440	1129.7500	-0.0060	-0.0064
CP_14	2447482.2446	322286.9030	1133.5990	1133.6000	-0.0010	-0.0014
CP_15	2447289.8486	322243.5513	1137.7390	1137.7300	0.0090	0.0086
CP_16	2447321.2590	322140.1606	1133.7420	1133.7500	-0.0080	-0.0084
CP_17	2447344.1892	322065.5780	1131.1530	1131.1800	-0.0270	-0.0274
CP_18	2447377.7205	321955.0422	1127.2000	1127.2200	-0.0200	-0.0204
CP_19	2447409.6357	321850.7671	1123.6010	1123.5200	0.0810	0.0806
CP_20	2447440.6037	321752.7325	1120.2160	1120.2100	0.0060	0.0056
CP_21	2447466.1464	321667.5136	1117.2100	1117.2600	-0.0500	-0.0504
CP_22	2447498.7418	321554.6298	1113.2700	1113.3100	-0.0400	-0.0404
CP_23	2447530.3931	321444.9524	1109.5140	1109.3400	0.1740	0.1736
CP_24	2447552.5875	321369.0845	1106.8410	1106.7800	0.0610	0.0606
CP_25	2447581.7572	321268.5857	1103.2270	1103.2500	-0.0230	-0.0234
CP_26	2447606.8815	321181.3414	1100.1830	1100.1500	0.0330	0.0326
CP_27	2447634.7895	321084.3153	1096.7430	1096.7200	0.0230	0.0226
CP_28	2447667.2819	320972.5669	1092.7720	1092.7900	-0.0180	-0.0184
				Number of Check Points	28	28
				Mean Error	0.000	0.000
				Standard Deviation (StDEV)	0.045	0.045
				Root Mean Squares Error ($RMSE_{x \text{ or } y \text{ or } z}$)	0.044	0.044
				NSSDA Vert Accuracy at 95% accuracy Level	0.086	
				NSSDA Vert Accuracy at 95% accuracy Level after z-bias removal	0.086	

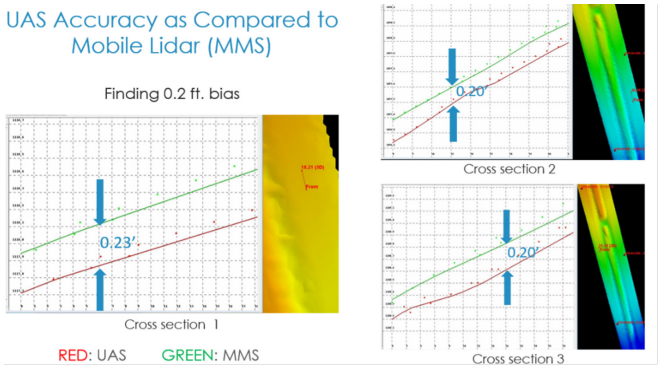

Figure 18: Bias in the photogrammetric DTM

Table 6: Vertical accuracy of UAS-based DTM as verified using MMS data

Point ID	MMS Elevation			UAS Elevation	Residual Values (ft.)	Delta Z after Z-bias Removed (ft.)
	Easting (ft.)	Northing (ft.)	Elevation (ft.)	Elevation (ft.)	Error in Elevation (ft.)	
CP_1	2447813.6658	320999.2773	1091.2600	1091.0900	0.1700	-0.0539
CP_2	2447783.7307	321113.7985	1095.1700	1094.9800	0.1900	-0.0339
CP_3	2447759.1650	321215.2972	1098.4000	1098.1600	0.2400	0.0161
CP_4	2447733.0793	321308.6243	1101.5000	1101.2200	0.2800	0.0561
CP_5	2447700.7566	321419.0448	1105.1900	1104.8700	0.3200	0.0961
CP_6	2447674.8168	321511.8570	1108.2900	1107.9800	0.3100	0.0861
CP_7	2447653.6632	321604.4581	1111.2300	1110.8400	0.3900	0.1661
CP_8	2447626.2922	321705.3985	1114.6300	1114.3200	0.3100	0.0861
CP_9	2447596.3534	321793.1424	1117.7100	1117.3800	0.3300	0.1061
CP_10	2447571.4603	321890.3933	1120.9300	1120.8700	0.0600	-0.1639
CP_11	2447546.6611	321995.9759	1124.4200	1124.2700	0.1500	-0.0739
CP_12	2447526.5566	322083.3588	1127.2400	1126.9900	0.2500	0.0261
CP_13	2447500.2614	322166.6011	1130.1800	1129.9000	0.2800	0.0561
CP_14	2447466.4229	322281.2289	1134.0600	1133.8900	0.1700	-0.0539
CP_15	2447308.6649	322248.5215	1138.2900	1138.0900	0.2000	-0.0239
CP_16	2447344.7171	322148.4501	1134.5300	1134.3400	0.1900	-0.0339
CP_17	2447365.3790	322069.0943	1131.7300	1131.6100	0.1200	-0.1039
CP_18	2447397.6980	321961.4341	1127.9300	1127.8300	0.1000	-0.1239
CP_19	2447432.4695	321852.6548	1124.1800	1124.1000	0.0800	-0.1439
CP_20	2447461.1104	321756.1124	1120.7400	1120.4600	0.2800	0.0561
CP_21	2447488.2891	321668.7552	1117.6600	1117.3400	0.3200	0.0961
CP_22	2447517.8379	321559.0553	1113.8200	1113.6100	0.2100	-0.0139
CP_23	2447551.4267	321449.0224	1110.0300	1109.8300	0.2000	-0.0239
CP_24	2447574.2564	321367.1508	1107.0900	1106.8800	0.2100	-0.0139
CP_25	2447603.1840	321268.4371	1103.5500	1103.2900	0.2600	0.0361
CP_26	2447630.6428	321182.1303	1100.5800	1100.4300	0.1500	-0.0739
CP_27	2447658.1476	321084.4832	1097.1100	1096.9100	0.2000	-0.0239
CP_28	2447691.2635	320973.0090	1093.2200	1092.9200	0.3000	0.0761
				Number of Check Points	28	28
				Mean Error	0.224	0.000
				Standard Deviation (StDEV)	0.083	0.083
				Root Mean Squares Error ($RMSE_{x \text{ or } y \text{ or } z}$)	0.238	0.081
				NSSDA Vert Accuracy at 95% accuracy Level	0.467	
				NSSDA Vert Accuracy at 95% accuracy Level after z-bias removal	0.159	

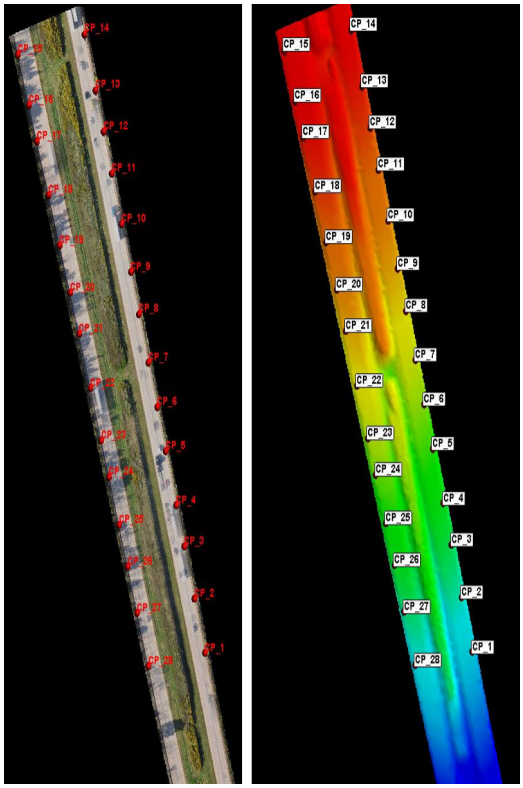

Figure 19: Checkpoint locations along SR80

Surveyed Checkpoints

PennDOT staff surveyed 28 independent checkpoints along the two sides of the highway using traditional leveling techniques (Figure 19). Table 7 lists the results of evaluating the UAS-based DTM using these independent checkpoints. Again, the surveyed checkpoints clearly verify the existence of the vertical bias in the UAS-based DTM as it was revealed by the MMS data. Once such bias is removed from the data, the vertical accuracy of the photogrammetric DTM was found to be around 0.095 feet (0.029 meters), which is in a close agreement with the MMS verification method.

Once the vertical bias is removed from the data, the accuracy results from the MMS-derived checkpoints align with those from the field-surveyed checkpoints. This agreement is a clear indication that MMS data is as accurate as the field-surveyed checkpoints.

Vertical biases are common in lidar data and can be estimated and removed as long as accurate ground control points are available within the project areas. Different from random errors, biases are systematic errors of a mathematical nature that can be modeled and removed from the data with the help of ground control points.

Additional verifications were performed by comparing the photogrammetric DTM to the DTM derived from MMS data. Contours generated from both technologies align horizontally and vertically within few tenths of a foot (Figure 20).

Table 7: UAS-based DTM vertical accuracy as verified using surveyed checkpoints

PennDOT UAS Proof of Concept - Accuracy Analysis (Comparing UAS DTM to PennDOT new check points)

Note: Elevation of check points were re-projected to Geoid 12B to match the vertical datum of the data

Point ID	Surveyed Elevation			UAS Elevation	Residual Values (ft.)	Delta Z after Z-bias Removed (ft.)
	Easting (ft.)	Northing (ft.)	Elevation (ft.)	Elevation (ft.)	Error in Elevation (ft.)	
CP_1	2447833.0894	321000.2444	1090.7890	1090.6120	0.1770	-0.0216
CP_2	2447802.1717	321113.8212	1094.5240	1094.3850	0.1390	-0.0596
CP_3	2447772.2693	321223.4371	1098.1050	1097.9650	0.1400	-0.0586
CP_4	2447748.5271	321310.1031	1100.9470	1100.8140	0.1330	-0.0656
CP_5	2447717.8919	321422.8742	1104.6990	1104.4980	0.2010	0.0024
CP_6	2447692.8522	321515.1178	1107.7650	1107.5460	0.2190	0.0204
CP_7	2447667.4935	321607.4306	1110.8140	1110.6590	0.1550	-0.0436
CP_8	2447639.9596	321708.4858	1114.1970	1114.0610	0.1360	-0.0626
CP_9	2447616.1907	321796.2994	1117.1080	1116.8630	0.2450	0.0464
CP_10	2447589.1547	321894.9876	1120.3930	1120.2970	0.0960	-0.1026
CP_11	2447560.6492	321999.9689	1123.9770	1123.7690	0.2080	0.0094
CP_12	2447536.9992	322086.5782	1126.8480	1126.7280	0.1200	-0.0786
CP_13	2447513.7209	322171.3742	1129.7440	1129.6260	0.1180	-0.0806
CP_14	2447482.2446	322286.9030	1133.5990	1133.3060	0.2930	0.0944
CP_15	2447289.8486	322243.5513	1137.7390	1137.5200	0.2190	0.0204
CP_16	2447321.2590	322140.1606	1133.7420	1133.6600	0.0820	-0.1166
CP_17	2447344.1892	322065.5780	1131.1530	1130.9820	0.1710	-0.0276
CP_18	2447377.7205	321955.0422	1127.2000	1127.0130	0.1870	-0.0116
CP_19	2447409.6357	321850.7671	1123.6010	1123.6410	-0.0400	-0.2386
CP_20	2447440.6037	321752.7325	1120.2160	1119.9360	0.2800	0.0814
CP_21	2447466.1464	321667.5136	1117.2100	1116.8400	0.3700	0.1714
CP_22	2447498.7418	321554.6298	1113.2700	1112.9910	0.2790	0.0804
CP_23	2447530.3931	321444.9524	1109.5140	1109.3450	0.1690	-0.0296
CP_24	2447552.5875	321369.0845	1106.8410	1106.5450	0.2960	0.0974
CP_25	2447581.7572	321268.5857	1103.2270	1102.8890	0.3380	0.1394
CP_26	2447606.8815	321181.3414	1100.1830	1099.9710	0.2120	0.0134
CP_27	2447634.7895	321084.3153	1096.7430	1096.5550	0.1880	-0.0106
CP_28	2447667.2819	320972.5669	1092.7720	1092.3410	0.4310	0.2324
	Number of Check Points				28	28
	Mean Error				0.199	0.000
	Standard Deviation (StDEV)				0.096	0.096
	Root Mean Squares Error ($RMSE_{x\,or\,y\,or\,z}$)				0.220	0.095
	NSSDA Vert Accuracy at 95% accuracy Level				0.431	
	NSSDA Vert Accuracy at 95% accuracy Level after z-bias removal				0.185	

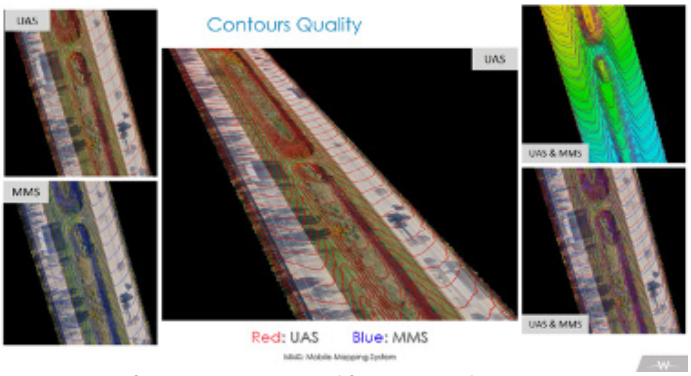

Figure 20: One-foot contours generated from MMS and stereo UAS imagery

Conclusion

As geospatial data quality and georeferencing are better defined and refined, fusing geospatial datasets derived from different sources becomes a routine matter. Users of geospatial data can reap the benefits of this reality. With demand for digital twins on the rise, geospatial data fusion is an ideal solution for providing seamless 3D models for projects and their surrounding areas.

This discussion demonstrated successful attempts to fuse different geospatial data to produce new, hybrid geospatial products with more potential to serve engineering projects than any of the individual products used in producing the final product. Combining disparate data sources requires careful communication about the data sources and data. Users must be aware that the hybrid product may have multiple accuracy levels depending on the data sources used in the generation of the new hybrid product. This can safely be accomplished through the metadata which needs to be closely attached to the new product.

This new approach is far more economical than current practices as it leverages existing data and enables effective utilization of UAS as an acquisition platform. Public domain geospatial data is increasingly available from state and county GIS websites. It provides tremendous relief to the project budget and schedule, and in most cases, it can be obtained instantaneously and free of charge.

In addition, this research proved that stereo pairs from UAS-based imagery can be used to support design-grade surveys for road engineering, assuming the UAS mission is planned and executed properly. UAS can be used in permissible areas (off roads and away from populated areas according to FAA regulations) to provide cost-effective products and replace countless hours of labor-intensive field surveying.

Finally, emerging geospatial technologies such as UAS are effective in serving transportation projects to help reduce costs and expedite delivery schedules. Using different technologies to serve projects with diverse specifications and requirements is the most efficient way to execute transportation projects as the hybrid approach contributes to better efficiency and resource utilization. Accuracy on demand within a project is a logical outcome of the hybrid approach.

Authors

Qassim Abdullah, Ph.D., PLS, CP, VP and Chief Scientist

As Woolpert's Chief Scientist, Qassim has more than 40 years of combined industrial, R&D and academic experience in analytical photogrammetry, digital remote sensing, and civil and surveying engineering. When he's not presenting at geospatial conferences around the world, Qassim teaches photogrammetry and remote sensing courses at the University of Maryland and Penn State, authors a monthly column for the ASPRS journal PE&RS, and mentors Woolpert's research and development activities.

Tom Ruschkewicz, Practice Leader, Transportation

Tom has 26 years of experience in the surveying and geospatial industry. A professional surveyor in four states, he has a diverse background encompassing public transportation, aviation, infrastructure, utilities, energy, telecommunications and residential/commercial land development. He has managed projects across the United States providing land surveying, geodetic control networks, lidar, aerial photogrammetry, ROW acquisition, UAS, subsurface utility engineering and other geospatial services.